

Towards CP -violation studies on superheavy molecules: Theoretical and experimental perspectivesR. Mitra ^{1,2}, V. S. Prasanna ³, R. F. Garcia Ruiz,⁴ T. K. Sato ⁵, M. Abe,⁶ Y. Sakemi ⁷, B. P. Das,^{3,8} and B. K. Sahoo¹¹*Atomic, Molecular and Optical Physics Division, Physical Research Laboratory, Navrangpura, Ahmedabad 380009, India*²*Indian Institute of Technology Gandhinagar, Palaj, Gandhinagar 382355, India*³*Centre for Quantum Engineering, Research and Education, TCG CREST, Salt Lake, Kolkata 700091, India*⁴*Department of Physics, Massachusetts Institute of Technology, Cambridge, Massachusetts 02139, USA*⁵*Advanced Science Research Center, Japan Atomic Energy Agency, Tokai, Ibaraki 319-1195, Japan*⁶*Department of Chemistry, Graduate School of Science, Hiroshima University, 1-3-2, Kagamiyama, Higashi-Hiroshima City, Hiroshima 739-8511, Japan*⁷*Center for Nuclear Study, The University of Tokyo, Hongo, Bunkyo, Tokyo 113-0033, Japan*⁸*Department of Physics, Tokyo Institute of Technology, 2-12-1 Ookayama, Meguro-ku, Tokyo 152-8550, Japan*

(Received 30 August 2021; revised 12 October 2021; accepted 16 November 2021; published 1 December 2021)

Molecules containing superheavy atoms can be artificially created to serve as sensitive probes to study symmetry-violating phenomena. Here, we provide detailed theoretical studies of quantities relevant to the electron electric dipole moment (eEDM) and nucleus-electron scalar-pseudoscalar interactions in diatomic molecules containing superheavy lawrencium nuclei. The sensitivity to parity and time (or, equivalently, CP) reversal violating properties is studied for different neutral and ionic molecules. The effective electric fields in these systems are found to be about 3–4 times larger than other known molecules on which eEDM experiments are being performed. Similarly, these superheavy molecules exhibit an enhancement of more than 3 times for CP -violating scalar-pseudoscalar nucleus-electron interactions. Our preliminary analysis using the Woods-Saxon nuclear model also demonstrates that these results are sensitive to the diffuse surface interactions inside the Lr nucleus. We also briefly comment on some experimental aspects by discussing the production of these systems.

DOI: [10.1103/PhysRevA.104.062801](https://doi.org/10.1103/PhysRevA.104.062801)**I. INTRODUCTION**

Recent advances in studies on heavy molecular systems are enabling new opportunities in fundamental physics [1–13]. Symmetry-violating properties of electrons, nuclei, and other fundamental particles and interactions between them can be highly enhanced in certain molecules [14,15]. Precision experiments using ThO, for example, have provided the most stringent bound on the electric dipole moment (EDM) of the electron [1], constraining the existence of new physics at the TeV scale [16]. The search for the electron and nuclear EDMs has attracted a great deal of experimental and theoretical attention because they are highly sensitive to new sources of time-reversal (T) violation (equivalent to CP violation) [15], knowledge of which can be useful in explaining the matter-antimatter asymmetry in the universe [17,18].

Paramagnetic molecules containing heavy nuclei are very interesting in view of their enhanced sensitivity to symmetry-violating phenomena. These enhancements were discussed in Ref. [19] for the atomic case and Ref. [20] for the case of diatomic molecules. In Ref. [21], the authors addressed the Z dependence of the electron EDM enhancement factor as $K = Z^3 R(Z\alpha)$, with the relativistic factor $R(Z\alpha)$ becoming very important for superheavy nuclei. We also note that the Z dependence of the CP -violating scalar-pseudoscalar (S-PS) nucleus-electron interactions was discussed in Ref. [22]. These developments motivate us to

consider diatomic molecules containing superheavy atoms for electron EDM studies. Future studies of these systems could open up new opportunities in fundamental physics and chemistry. There have been recent advances in the search for the electron EDM using paramagnetic molecules, which would be a signature of CP violation beyond the standard model of elementary particles. Moreover, spectroscopic results from studies of superheavy elements were recently reported, and in view of these developments, it is desirable to investigate EDMs using molecules with superheavy atoms. However, our experimental knowledge of such rare molecules is in its infancy, and theoretical developments are critical to motivate and guide experimental progress [23,24].

Within a molecule, the magnitude of the intrinsic electric field that an electron with an EDM experiences due to the other electrons and nuclei can be viewed as an effective electric field \mathcal{E}_{eff} [19]. Because of their large atomic number, superheavy radioactive elements are expected to exhibit a substantial enhancement in their \mathcal{E}_{eff} since one expects relativistic and electron correlation effects to be prominent. Indeed, effective electric fields of CnH [25,26], CnF [27], LrO, NoF, RfN, E120F (where E120 stands for element 120), and E121O (where E121 stands for element 121) [28] have been calculated and attest to the above statement. In this work, we focus our studies on diatomic molecules containing Lr atoms, i.e., LrO, LrF⁺, and LrH⁺. Because of their short half-lives and low production rates, superheavy elements, including Lr, need

to be handled on a single-atom scale. There are 14 different isotopes of Lr, of which we propose to employ ^{256}Lr (half-life ≈ 27 s), which has been used in several studies of atomic properties. A purified single ion beam of ^{256}Lr , synthesized in the ^{249}Cf (^{11}B , $4n$) reaction, was successfully produced by using the Isotope Separator On-Line (ISOL) system at the Tandem accelerator facility of the Japan Atomic Energy Agency (JAEA) [29]. We explore a possible alternative scheme to produce Lr atoms. Our work also aims to extend the studies of molecular ions, which could enable precision measurements with just a single molecular ion [30–32].

This paper is organized as follows: Sec. II presents the general theory of molecular EDMs due to electron EDM and S-PS nucleus-electron interactions. The many-body method employed in the present work is explained in Sec. III. Our theoretical results and a discussion of the sensitivity of these molecules to symmetry-violating properties are presented in Sec. IV.

II. THEORY

Theoretical studies on their sensitivity to symmetry-violating properties were performed for the diatomic molecules LrO , LrF^+ , and LrH^+ . We employed a four-component relativistic coupled-cluster (RCC) method for this purpose. The fully relativistic aspect becomes especially relevant, as theoretical calculations have predicted that the Lr atom would have a configuration different from that expected by a nonrelativistic treatment, $[\text{Rn}]5f^{14}6d^17s^2$, due to strong relativistic effects [33]. The $[\text{Rn}]5f^{14}7s^27p_{1/2}$ configuration would be most probable for the Lr atom according to the measurement of the first ionization potential [29]. We employ the configuration for calculations in the present work. Since LrO , LrF^+ , and LrH^+ have one unpaired electron each, these molecules are sensitive to both the electron EDM and nucleus-electron S-PS interactions [34]. Thus, these T -odd sources can induce an energy shift (approximated only to first order) in the molecular levels given by

$$\Delta E \simeq \Delta E^{(1)} = -d_e \mathcal{E}_{\text{eff}} + k_s W_s, \quad (1)$$

where the first term on the right-hand side of Eq. (1) describes the contribution from the electron EDM and the second term shows that from the S-PS interaction. In the above equation, k_s is the coupling parameter for the S-PS interaction, with the accompanying quantity W_s being the analog of \mathcal{E}_{eff} , and like the effective electric field, it too can be calculated only by using many-body theory. The calculation of \mathcal{E}_{eff} and W_s , in combination with the measured value of ΔE , can provide upper bounds on d_e and k_s .

The interaction Hamiltonian due to the electron EDM in a molecule is given by [35]

$$\begin{aligned} H_{\text{EDM}} &= -2icd_e \sum_{j=1}^{N_e} \beta \gamma_5 p_j^2 \\ &= \sum_{j=1}^{N_e} h_{\text{EDM}}(r_j), \end{aligned} \quad (2)$$

where c is the speed of light, β is a Dirac matrix, γ_5 is the product of Dirac matrices, p_j is the momentum operator

corresponding to the j th electron, and N_e is the total number of electrons in the system. Assuming that the shift in energy is due to only the electron EDM, the expression for \mathcal{E}_{eff} can be obtained as

$$\mathcal{E}_{\text{eff}} = -\frac{1}{d_e} \frac{\langle \Psi | H_{\text{EDM}} | \Psi \rangle}{\langle \Psi | \Psi \rangle}, \quad (3)$$

where $|\Psi\rangle$ is the ground-state wave function of the molecule. Similarly, the S-PS interaction Hamiltonian manifesting at the molecular level is given by [35–37] $H_{\text{S-PS}} = \sum_{A=1}^{N_{\text{nuc}}} H_{\text{S-PS},A}$, with

$$H_{\text{S-PS},A} = i \frac{G_F}{\sqrt{2}} k_{s,A} M_A \sum_{j=1}^{N_e} \beta \gamma_5 \rho_A(r_{A,j}), \quad (4)$$

where A denotes the A th nucleus; $M_A = Z_A + N_A$ is the mass number of the A th nucleus, with Z_A being the number of protons and N_A being the number of neutrons; ρ_A is the nuclear charge density normalized to unity (i.e., the average nucleon density; we assume that the nucleon number density of the nucleus and the nuclear charge density are proportional); $G_F = 2.219 \times 10^{-14}$ (in atomic units) is the Fermi coupling constant; N_{nuc} is the total number of nuclei in the molecule; and $k_{s,A}$ is the S-PS coupling coefficient of the corresponding nucleus, A . We have accounted here for only the contribution from the heaviest atom (since the contribution from the heavier of the two atoms dominates) and denote $k_{s,A}$ as k_s for brevity. The quantity of theoretical interest in the S-PS interaction, W_s , is given by

$$W_s = \frac{1}{k_s} \frac{\langle \Psi | H_{\text{S-PS}} | \Psi \rangle}{\langle \Psi | \Psi \rangle}. \quad (5)$$

It is worth mentioning that in the considered Lr isotopes, the numbers of protons and neutrons are not the same. Thus, ρ_A will be different for the proton and neutron distributions, leading to slight changes in the results. These corrections can be estimated through neutron skin effects with the knowledge of nucleon wave functions and have been neglected in this work.

Another property that plays an important role in determining the statistical sensitivity of a molecule in an EDM experiment is the molecular permanent electric dipole moment (PDM). The PDM can be evaluated as the expectation value of the electric dipole operator and is given as

$$\begin{aligned} \mu &= \langle \Psi | \left(\sum_{A=1}^{N_{\text{nuc}}} Z_A R_A - \sum_{i=1}^{N_e} r_i \right) | \Psi \rangle \\ &= \mu_{\text{nuc}} - \mu_e, \end{aligned} \quad (6)$$

where R_A and r_i are, respectively, the positions of the A th nucleus and i th electron with respect to the origin. Since we employ the Born-Oppenheimer approximation [38], where the nuclei are clamped, R_A are constants and are determined from the minimum of the potential-energy surface for a given molecule. In the expression, μ_{nuc} and μ_e are the nuclear and electronic contributions to PDM, respectively. Since the investigated molecules are diatomic systems, each of the systems has only one equilibrium bond length R_e . We have set the Lr atom as the origin to define R_e . Therefore, the PDMs of the charged systems are specified with Lr as the origin.

We add here that it is straightforward to obtain the PDM at any other origin, including setting it at the center of mass of the molecular system, as the property simply scales with the change in origin.

Owing to the fact that atoms are spherically symmetric, their EDMs are more relevant quantities for theoretical studies than effective electric fields. Analogous to Eq. (1), the EDM of an atom d_A can be given as [19–21]

$$d_A = \langle D \rangle = d_e \mathcal{R} + k_s \mathcal{S}, \quad (7)$$

where \mathcal{R} and \mathcal{S} are known as the enhancement factors to d_A due to d_e and k_s , respectively.

III. METHOD OF CALCULATION

The molecular parameters were calculated by solving the many-body wave function of the molecular system within a relativistic framework. To account for the relativistic and electron correlation effects rigorously, we employ here the RCC theory, expressing the wave function as [39]

$$|\Psi\rangle = e^T |\Phi_0\rangle, \quad (8)$$

where $|\Phi_0\rangle$ is the Dirac-Hartree-Fock (DHF) wave function and T is the cluster operator. The latter is responsible for generating particle-hole excitations which arise out of the DHF state due to the residual Coulomb interaction that is ignored in the evaluation of the DHF wave function. T is expressed as

$$T = T_1 + T_2 + T_3 + \dots + T_{N_e}, \quad (9)$$

where the operator T_i accounts for all possible i particle– i hole excitations. Due to the prohibitively expensive cost associated with including all the excitations, we adopt the common practice where one restricts T to include only single and double excitations (RCCSD method), in which the excitation operators are defined using the second quantization operators as

$$T_1 = \sum_{i,a} t_i^a a_a^\dagger a_i \quad (10)$$

and

$$T_2 = \frac{1}{4} \sum_{i,j,a,b} t_{ij}^{ab} a_a^\dagger a_b^\dagger a_i a_j, \quad (11)$$

where the indices i, j, k , etc., denote the occupied orbitals and a, b, c, \dots identify the virtual orbitals, t_i^a is the amplitude for a single excitation from i th occupied orbital to the a th virtual orbital, and t_{ij}^{ab} is the amplitude of the double excitation from the occupied i and j orbitals to the virtual a and b orbitals, respectively.

Once the ground-state wave function of a molecule is obtained, we calculate the properties of interest by using the expectation-value approach. The expectation value of an operator O in the RCC method is given by

$$\begin{aligned} \langle O \rangle &= \frac{\langle \Phi_0 | e^{T^\dagger} O e^T | \Phi_0 \rangle}{\langle \Phi_0 | e^{T^\dagger} e^T | \Phi_0 \rangle} \\ &= \langle \Phi_0 | e^{T^\dagger} O e^T | \Phi_0 \rangle_l, \end{aligned} \quad (12)$$

where the subscript l means that only the linked terms contribute. In the RCCSD method, since $T \simeq T_1 + T_2$, we

have

$$\begin{aligned} \langle O \rangle &= \langle \Phi_0 | O | \Phi_0 \rangle_l + \langle \Phi_0 | (OT_1 + \text{H.c.}) + T_1^\dagger OT_1 + T_2^\dagger OT_2 \\ &\quad + \frac{1}{2}(T_1^\dagger OT_1^2 + \text{H.c.}) + \frac{1}{2}(T_2^\dagger OT_1^2 + \text{H.c.}) \\ &\quad + (T_2^\dagger OT_1 T_2 + \text{H.c.}) + \dots | \Phi_0 \rangle_l, \end{aligned} \quad (13)$$

where H.c. stands for the Hermitian conjugate term [40,41]. It can be noted that OT_2 and its H.c. term do not give us fully contracted terms owing to the one-body form of the operators, which describes the properties that are investigated here; that is, O is the PDM operator, and H_{EDM} and $H_{\text{S-PS}}$ are used for the evaluation of μ , \mathcal{E}_{eff} , and W_s . In the above expression, the first term gives the DHF value, and the OT_1 term includes electron correlations arising through the core-polarization and pair-correlation effects to all orders. Therefore, it contributes dominantly to the electron correlation effects.

IV. RESULTS AND DISCUSSION

At the outset, it is critical to find whether the systems of interest can form bound states. The ground-electronic-state energies at several bond lengths were calculated to construct the potential-energy curve (PEC) of each molecule. We then identify the minimum of the PEC, whose corresponding bond length provides the molecular R_e . We carry out this procedure for LrO, LrF⁺, and LrH⁺ (Fig. 1) while ensuring that for each molecule, we choose more grid points around the minimum to pinpoint R_e to an accuracy of two decimal places in atomic units. We employ the RCCSD method with the inclusion of partial triple excitations in a perturbational manner, using the DIRAC 18 package [42,43]. This approach is referred to as the RCCSD(T) method. We use Dyal’s triple-zeta (TZ) v3z [44] basis sets. To lower the computational requirements while compromising little on accuracy, we have cut off the high-lying virtual orbitals with energies above 2000 a.u. The value of R_e for LrO was found to be 3.46 a.u., while that of LrF⁺ and LrH⁺ was found to be 3.56 a.u. The PECs of each of the molecules exhibit a smooth trend with a clear global minimum (see Fig. 1).

After finding the equilibrium bond lengths of the investigated molecules, we calculate the other properties of interest. For this purpose, we use Dyal’s quadruple-zeta (QZ) v4z [44] basis sets. We employ the UTCHEM [45,46] package for DHF calculations and for atomic orbital to molecular orbital integral transformations and, in tandem, use the DIRAC08 package for RCC calculations [47]. We finally use our expectation-value code to evaluate the values of the properties [48]. We present the calculated values of \mathcal{E}_{eff} , W_s , their ratios, and μ of LrO, LrF⁺, and LrH⁺ from the DHF and RCCSD methods in Table I. We also compare our results for LrO with the only available values in literature from Refs. [28,49]. In Ref. [28], the authors used (37s, 34p, 14d, and 9f) uncontracted Gaussian-type functions for Lr and a decontracted atomic-natural-orbital basis set of TZ quality for O. They performed their calculations by employing the complex generalized Hartree-Fock (cGHF) and complex generalized Kohn-Sham (cGKS) theories. They obtained R_e of 3.51 and 3.53 a.u. with the cGHF and the cGKS approaches, respectively, which is in reasonably close proximity to our estimated value of 3.46 a.u. The value of \mathcal{E}_{eff} using the cGHF method

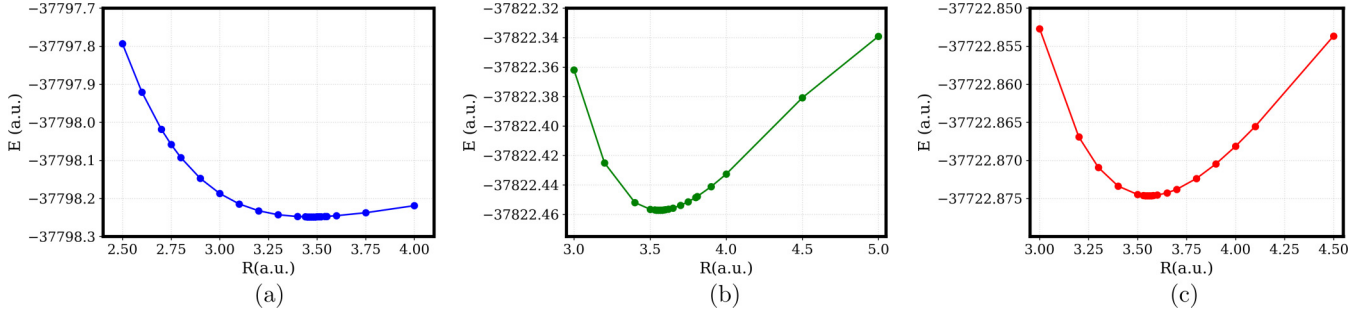


FIG. 1. Potential-energy curves of (a) neutral LrO and (b) LrF⁺ and (c) LrH⁺ molecular ions with a range of typical molecular bond lengths R using the RCCSD(T) method. The plots show that LrO can form a stable molecule around the equilibrium bond length $R_e \simeq 3.46$, while both the ions have minima around $R_e \simeq 3.56$. All the values are given in atomic units.

came out to be 322.58 GV/cm, while the cGKS method yielded 250.21 GV/cm. Our calculation, using the RCCSD method and with Dyall's QZ bases for Lr (37*s*, 34*p*, 24*d*, and 14*f*) and O (18*s* and 10*p*), gives an \mathcal{E}_{eff} of 258.92 GV/cm and is in better agreement with their results from the cGKS method than from the cGHF approach.

In Ref. [49], the authors used analytic first derivatives for exact two-component CCSD and CCSD(T) methods and employed TZ quality basis sets. Further, they froze several of the occupied orbitals in their computations and obtained an effective electric field of 263.9 GV/cm with CCSD and 246.5 GV/cm with the CCSD(T) approach. Although their CCSD results are in reasonable agreement with our CCSD results obtained using all-electron fully relativistic CCSD calculations and with a QZ basis, this agreement could be fortuitous. This is evident from the disagreement in the correlation trends in Ref. [49], where the DHF result is greater than that of the CCSD counterpart. In Table I, we also compare our results with the corresponding values for ThO, for which the most accurate EDM measurement is available, and HgF, which possesses the largest \mathcal{E}_{eff} estimated thus far for nonsuperheavy systems. The Lr molecules were found to have

values of \mathcal{E}_{eff} that are 3–4 times larger than those of ThO and HgF [2,8]. Similarly, the values of W_s for LrO and LrF⁺ were found to be about 4 times larger than that for HgF. Table I also provides the values for these quantities for other leading candidates, HfF⁺ and YbF [50,51]. Additionally, Table I provides data on the ratio of W_s and \mathcal{E}_{eff} . The significance of the quantity is related to the fact that one needs to perform two experiments to extract both the electron EDM and the S-PS interaction, as seen from Eq. (1). We also present \mathcal{R} , \mathcal{S} , and their ratios for the leading atomic candidates, Cs, Tl, Rb, and Fr, from the literature [52–55] in Table I.

In Table II, we present contributions to the values of \mathcal{E}_{eff} , W_s , and μ for LrO, LrF⁺, and LrH⁺ from different terms of the RCCSD method, given in Eq. (13). The first term corresponds to the DHF value, while the other terms represent correlation contributions. As Table II shows, $OT_1 + \text{H.c.}$ terms contribute the most to the correlation effects. We note at this point that OT_1 primarily contains correlation effects arising from the interaction of pairs of electrons. $T_1^\dagger OT_1$ also contains effects involving pairs of electrons, but the interplay between the EDM and Coulomb interactions is more complex. The next-leading-order contributions arise from $T_1^\dagger OT_1$. Al-

TABLE I. Calculated values of \mathcal{E}_{eff} , W_s (with $M_A = 256$), and μ for LrO, LrF⁺, and LrH⁺ using the RCCSD method and comparison with literature values when they are available. We also compare these values with calculations of the corresponding quantities for other molecules and atoms (see the text for further details). Note that in the literature values given for molecules, the authors used Z_A in place of M_A in the definition of W_s , and we have multiplied by M_A/Z_A to rescale those values to be consistent with the definition adopted in the present work.

Molecule	\mathcal{E}_{eff} (GV/cm)	W_s (kHz)	$W_s/\mathcal{E}_{\text{eff}}$ (kHz cm/GV)	$W_s/\mathcal{E}_{\text{eff}}$ ($10^{-21} e \text{ cm}$)	μ (D)	Reference
LrO	258.92	2565.54	9.91	41.03	4.58	This work
	250.21	2367.77	9.46	39.16		[28]
	246.5					[49]
LrF ⁺	246.31	2445.83	9.93	41.11	12.29	This work
LrH ⁺	343.38	3402.36	9.91	41.03	11.05	This work
ThO	87	300.24	3.45	14.29	4.27	Ref. [2]
HgF	115.42	668.37	5.79	23.97	3.96	Ref. [8,27]
HfF ⁺	22.5	49.41	2.20	9.11		[50]
YbF	23.2	100.67	4.34	17.97	3.91	[51]
Atom	\mathcal{R}	\mathcal{S} ($10^{-18} e \text{ cm}$)		\mathcal{S}/\mathcal{R} ($10^{-21} e \text{ cm}$)		Reference
Cs	120.53	0.80		6.64		[52,53]
Tl	558	6.77		12.13		[54]
Rb	25.74	0.11		4.27		[52]
Fr	812.19	10.62		13.08		[55]

TABLE II. Contributions from the individual terms of the expectation-value expression in the RCCSD method to \mathcal{E}_{eff} , W_s , and μ for LrO, LrF⁺, and LrH⁺. The trends in different contributions between \mathcal{E}_{eff} and W_s are shown.

Term	\mathcal{E}_{eff} (GV/cm)			W_s (kHz)			μ (D)		
	LrO	LrF ⁺	LrH ⁺	LrO	LrF ⁺	LrH ⁺	LrO	LrF ⁺	LrH ⁺
O	235.16	215.20	283.59	2346.95	2149.75	2821.54	-898.40	-828.32	-919.79
$OT_1 + \text{H.c.}$	65.02	35.52	76.06	632.20	348.28	746.75	-1.62	-0.56	-0.72
$T_1^\dagger OT_1$	-26.28	-2.24	-9.56	-262.64	-22.42	-96.71	-0.59	-0.09	-0.14
$T_1^\dagger OT_2 + \text{H.c.}$	-8.11	-2.87	0.95	-82.72	-29.38	-81.92	0.58	0.14	0.12
$T_2^\dagger OT_2$	-8.54	-1.70	-8.21	-85.57	-17.05	9.27	-0.48	-0.14	-0.14
Other terms	1.67	2.4	-0.45	17.32	16.65	3.43	-0.44	0.08	0.02
Nuclear term							905.56	841.27	931.73
Total	258.92	246.31	343.38	2565.54	2445.83	3402.36	4.58	12.29	11.05

though the terms related to the T_2 operator give comparatively small contributions, they are non-negligible. In fact, for LrO, a sizable number of the contributions from $OT_1 + \text{H.c.}$ terms are canceled out by the other terms that are linear in T . The row denoted ‘‘Other terms’’ shows that the nonlinear terms are negligible even for the considered superheavy systems. Comparisons between the ratios of the magnitudes of $OT_1 + \text{H.c.}$ and DHF values of \mathcal{E}_{eff} , W_s , and μ in LrO, which come out to be ≈ 0.28 , ≈ 0.27 , and ≈ 0.23 , respectively, indicate that the electron correlation effects are almost equally important in all these quantities. Similarly, for \mathcal{E}_{eff} , W_s , and μ , we find these ratios to be ≈ 0.16 , ≈ 0.16 , and ≈ 0.27 , respectively, for LrF⁺ and ≈ 0.27 , ≈ 0.17 , and ≈ 0.26 , respectively, for LrH⁺. These results suggest that the electron correlation trends are almost the same in both molecular ions.

We now briefly comment on the molecular orbital information in the chosen systems. We expect that the singly occupied molecular orbital (SOMO) electron is localized in the s orbital of Lr for the following reasoning: Lr has a $7s^2 7p^1$ configuration, while O, H⁺, and F⁺ are expected to pull two electrons towards themselves owing to their larger electronegativity, thus leading to Lr $7s^1$. We verified this reasoning explicitly by examining the atomic components of the SOMO for all three systems and, indeed, found that the atomic orbitals from Lr provide the dominant contributions. We also carried out population analysis and found that in LrF⁺, for example, the SOMO is predominantly made out of the s function of Lr (0.86), followed by its d (0.09) and p functions (0.0388).

As seen in Table II, the major contribution to the properties of interest in this work comes from the DHF part. Therefore, we take a closer look at the DHF contribution in order to understand the possible reasons for observing large values of \mathcal{E}_{eff} and W_s in the studied superheavy molecules compared to other systems. Typically, in these molecules, the heavier atom provides most of the contributions to \mathcal{E}_{eff} and W_s . Due to the short-range and odd-parity nature of the scalar interaction Hamiltonians, the $s_{1/2}$ and $p_{1/2}$ orbitals generally contribute predominantly to \mathcal{E}_{eff} and W_s . It is known that relativistic effects deform the inner core orbitals, $s_{1/2}$ and $p_{1/2}$, strongly in the heavier atomic system. Thus, it is anticipated that these orbitals can strongly influence the \mathcal{E}_{eff} and W_s values in LrO, LrF⁺, and LrH⁺. We explicitly verify this argument by decomposing the DHF contribution to \mathcal{E}_{eff} (we do not repeat the analysis for W_s , as we expect trends similar to the effective

electric field for it) for all the three systems as

$$\begin{aligned}
 \mathcal{E}_{\text{eff}}^{\text{DHF}} &= \frac{1}{d_e} \langle \Phi_0 | H_{\text{EDM}} | \Phi_0 \rangle \\
 &= \frac{1}{d_e} \sum_j \langle \phi_j | h_{\text{EDM}} | \phi_j \rangle \\
 &= \frac{1}{d_e} \langle \phi_v | h_{\text{EDM}} | \phi_v \rangle \\
 &= \frac{1}{d_e} \sum_k \sum_l C_k C_l \langle \chi_{v,k} | h_{\text{EDM}} | \chi_{v,l} \rangle. \quad (14)
 \end{aligned}$$

In the above expression, the sum over all MO contributions boils down to only the valence molecular orbital (SOMO, denoted as v in the above set of equations) term because contributions from orbitals with opposite spin components of the closed-shell configuration cancel each other out. In the last line, we have expanded the valence molecular orbital as the sum of atomic orbitals (AOs) $|\chi_{v,i}\rangle$, where i can be l or k . Further details about this decomposition of SOMO to AOs can be found in, for example, Ref. [56]. Note that the SOMO contains contributions from both constituent atoms of a molecule. Of all the terms in Eq. (14), the contributions from the s and $p_{1/2}$ orbitals of Lr dominate and account for about 232, 214, and 281 GV/cm for LrO, LrF⁺, and LrH⁺, respectively, as shown in Fig. 2. Note that the DHF values for these systems are 235, 215, and 284 GV/cm for LrO, LrF⁺, and LrH⁺, respectively. The other contributions, such as those from $p_{3/2}$ and $d_{3/2}$ of Lr, s and $p_{1/2}$ of the lighter atom, etc., are less than 1 GV/cm. It is also worth noting that while the DHF values of LrO and LrH⁺ themselves are different by only about 50 GV/cm, the total effective electric fields are different by more than 80 GV/cm. This is attributed to the significant cancellation between the $OT_1 + \text{H.c.}$ and the $T_1^\dagger OT_1$ terms in LrO, as shown in Table II.

We would like to mention here that the above calculations were carried out by assuming Gaussian nuclear charge distribution. Since Gaussian-type functions are used to construct the MOs, it was convenient to consider the Gaussian nuclear charge distribution in the calculations [57]. Because Lr is a superheavy radioactive element, its nuclear charge distribution may be explained more accurately by using a more realistic nuclear charge distribution such as the Fermi [58] or Woods-Saxon [59,60] charge distribution. In order to get an

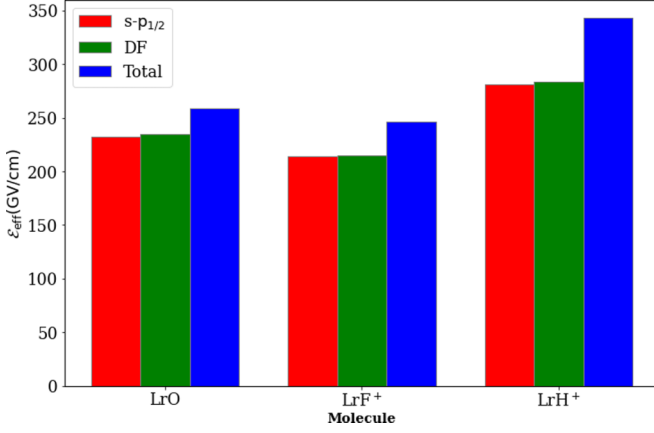


FIG. 2. Bar plots showing effective electric fields of LrO, LrF⁺, and LrH⁺ at three levels: The s - $p_{1/2}$ mixing contributions from Lr at the DHF level of theory (left bars), the DHF values themselves (middle bars), and the total values (right bars). All units are in gigavolts per centimeter.

impression about how the results differ by considering different nuclear charge-distribution models in the Lr isotopes, we investigate below the EDM enhancement factors, \mathcal{R} and \mathcal{S} , in two isolated isotopes of Lr due to d_e and k_S using various forms of nuclear charge distributions and potentials.

In the pointlike nuclear model, the nuclear density is $\rho_A(0) = 0$, and the nuclear potential takes the form

$$V(r) = -\frac{Z_A}{r}. \quad (15)$$

In the simplest case, one can assume uniform nuclear charge density in which the nuclear density and potential are

$$V(r) = -\frac{Z_A}{\mathcal{N}r} \times \begin{cases} \frac{1}{c} \left[\frac{3}{2} + \frac{a^2 \pi^2}{2c^2} - \frac{r^2}{2c^2} + \frac{3a^2}{c^2} P_2^+ + \frac{6a^3}{c^2 r} (S_3 - P_3^+) \right] & \text{for } r_i \leq c, \\ \frac{1}{r_i} \left[1 + \frac{a^2 \pi^2}{c^2} - \frac{3a^2 r}{c^3} P_2^- + \frac{6a^3}{c^3} (S_3 - P_3^-) \right] & \text{for } r_i > c, \end{cases} \quad (21)$$

where the factors are

$$\begin{aligned} \mathcal{N} &= 1 + \frac{a^2 \pi^2}{c^2} + \frac{6a^3}{c^3} S_3, \\ S_k &= \sum_{l=1}^{\infty} \frac{(-1)^{l-1}}{l^k} e^{-lc/a}, \\ P_k^{\pm} &= \sum_{l=1}^{\infty} \frac{(-1)^{l-1}}{l^k} e^{\pm l(r-c)/a}. \end{aligned} \quad (22)$$

In the Woods-Saxon model, the nuclear charge density is again given by using a uniform charge distribution but using different rms radii for protons and neutrons:

$$\rho_n(r) = \rho_0^n \Theta \left(1 - \frac{r}{R_n} \right), \quad (23)$$

with the corresponding normalization constant $\rho_0 = 3Z_A/4\pi R_n^3$ for $R_n = r_0^n M_A^{1/3}$. We have taken $r_0^n = 1.275$ fm and $r_0^n = 1.347$ fm for protons and neutrons, respectively [62]. Therefore, the Coulomb potential due to this charge

given by

$$\rho_A(r) = \rho_0 \Theta \left(1 - \frac{r}{R_A} \right) \quad (16)$$

and

$$V(r) = \begin{cases} -\frac{3Z_A}{2R_A^{\text{rms}}} \left[1 - \frac{1}{3} \left(\frac{r}{R_A^{\text{rms}}} \right)^2 \right] & \text{for } r \leq R_A^{\text{rms}}, \\ -\frac{Z_A}{r} & \text{for } r > R_A^{\text{rms}}, \end{cases} \quad (17)$$

where $\rho_0 = 3Z_A/4\pi R_A^3$ is the normalization constant, R_A is the radius of an arbitrary sphere in which nuclear charges are distributed, and R_A^{rms} is the rms radius of the A th nucleus. Θ is the Heaviside step function. We have determined $R_A = r_0 M_A^{1/3}$, with $r_0 = 1.2$ fm, M_A being the atomic mass, and $R_A^{\text{rms}} = \sqrt{(3/5)} R_A$.

In the Gaussian nuclear charge-distribution model, the nuclear density is given by

$$\rho_A(r) = \left(\frac{\eta_A}{\pi} \right)^{3/2} e^{-\eta_A r^2}, \quad (18)$$

with $\eta_A = \frac{3}{2} (R_A^{\text{rms}})^{-2}$, where R_A^{rms} is the rms nuclear charge radius of the A th nucleus. This leads to the expression for the nuclear potential observed by an electron:

$$V(r) = -\frac{Z_A}{r} \text{erf}(\sqrt{\eta} r). \quad (19)$$

Similarly, the Fermi nuclear charge distribution is given by

$$\rho_A(r) = \frac{\rho_0}{1 + e^{(r-c)/a}}, \quad (20)$$

where ρ_0 is the normalization constant, c is the half-charge radius, and $a = 2.3/4 \ln(3)$ is known as the skin thickness. The expression for the nuclear potential in this case is given by [61]

distribution can be given by

$$V_C^n(r) = \begin{cases} -\frac{3Z_A}{2R_n^{\text{rms}}} \left[1 - \frac{1}{3} \left(\frac{r}{R_n^{\text{rms}}} \right)^2 \right] & \text{for } r \leq R_n^{\text{rms}}, \\ -\frac{Z_A}{r} & \text{for } r > R_n^{\text{rms}}. \end{cases} \quad (24)$$

In addition to the Coulomb interaction, the Woods-Saxon model takes care of corrections to the nuclear potential due to diffuse surface (V_{ds}^n) and spin-orbit (V_{ls}^n) interactions. This results in a net nuclear potential given by [59,60]

$$V(r) = V_C^n(r) + V_{ds}^n(r) + V_{ls}^n(r), \quad (25)$$

where $V_{ds}^n = V_0 f_{ds}^n(r)$, with $a' = 0.65$ fm, $R_n^{\text{rms}} = r_0^n M_A^{1/3}$ fm, and

$$f_{ds}^n(r) = \begin{cases} \frac{1}{1 + e^{(r-R_n^{\text{rms}})/a'}} & \text{for } r \leq R_n^{\text{rms}}, \\ 0 & \text{for } r > R_n^{\text{rms}}, \end{cases} \quad (26)$$

and

$$V_{ls}^n(r) = V_{ls}^c r_0^n \mathbf{L} \cdot \mathbf{S} \frac{1}{r} \frac{df_{ls}^n(r)}{dr} \quad (27)$$

TABLE III. The enhancement factors for the isolated Lr isotopes, ^{253}Lr and ^{255}Lr , due to d_e and k_s , considering various nuclear charge-density distributions using the DHF method. In the Woods-Saxon model, results indicated for “Coulomb” refer to Coulomb interaction contributions, while the revised values after adding corrections for diffuse surface and spin-orbit interactions are given as “+Surface diffuse” and “+LS,” respectively.

Model	\mathcal{R}	\mathcal{S} ($10^{-18} e \text{ cm}$)
^{253}Lr isotope		
Pointlike	−2091.39	0.0
Uniform	−1628.51	−31.74
Gaussian	−1638.11	−33.18
Fermi	−1631.06	−32.28
Woods-Saxon		
Coulomb	−1608.66	−31.20
+Surface diffuse	−1420.18	−15.18
+LS	−1403.27	−15.45
^{255}Lr isotope		
Pointlike	−2091.39	0.0
Uniform	−1627.66	−31.71
Gaussian	−1637.35	−33.40
Fermi	−1630.29	−32.48
Woods-Saxon		
Coulomb	−1607.79	−31.17
+Surface diffuse	−1420.40	−15.18
+LS	−1414.60	−15.25

for the orbital angular momentum operator \mathbf{L} , spin operator \mathbf{S} , $V_{ls}^c = 0.44V_0^n$, and

$$f_{ls}^n(r) = \begin{cases} \frac{1}{1+e^{-(r-R_n^{ls})/d}} & \text{for } r \leq R_n^{ls}, \\ 0 & \text{for } r > R_n^{ls}, \end{cases} \quad (28)$$

with $R_n^{ls} = r_{ls}^n M_A^{1/3}$. We have taken $r_{ls}^n = 0.932$ fm and $r_{ls}^n = 1.280$ fm for protons and neutrons, respectively [62]. In the above expressions, V_0^n are chosen to be $V_0^n = 51 + 33(N_A - Z_A)/(N_A + Z_A)$ MeV and $V_0^n = 51 - 33(N_A - Z_A)/(N_A + Z_A)$ MeV for protons and neutrons, respectively.

Although earlier we suggested considering ^{256}Lr in the experiment, we consider here the ^{253}Lr and ^{255}Lr odd isotopes to analyze the spin-orbit effects. It can be noticed that other contributions from the aforementioned models, except the spin-orbit interactions, will be almost similar in the calculations of \mathcal{R} and \mathcal{S} . According to shell-model configurations, these isotopes have an odd proton in the valence orbitals (in the $f_{7/2}$ orbital for ^{253}Lr and in the $p_{1/2}$ orbital for ^{255}Lr) [63,64]. The dependences of these charge-distribution models on the estimation of \mathcal{E}_{eff} come indirectly through $V(r)$, while evaluation of W_s depends both directly and indirectly on it. Since this exercise is carried out to demonstrate the influence in the results due to the choice of different nuclear distribution models, we have employed the DHF method for this purpose, and the results are given in Table III. As can be seen in Table III, there are a significant differences in the results when a finite-size nucleus is considered over the point nucleus. The results do not differ substantially when different nuclear charge-distribution models are considered, but a large effect is seen when the diffuse surface interaction is introduced. The

results do not change significantly due to the spin-orbit interactions. Also, differences between the results for the ^{253}Lr and ^{255}Lr isotopes are negligibly small. This analysis suggests that the W_s values of the considered molecules may decrease by $\sim 40\%$ if the calculations are carried out by introducing the diffuse potential, which we defer to future work.

Using the values of the PDM and bond length of a molecule, we estimate the polarizing electric field for that system, which is given by $E_{\text{pol}} = \frac{2B}{\mu}$, with B being the rotational constant. The E_{pol} of LrO is 18.38 kV/cm, while it is 5.79 and 101.03 kV/cm for LrF^+ and LrH^+ , respectively. The E_{pol} required to polarize LrO and LrF^+ are practically achievable in the laboratory. The larger, and thus less desirable, value of E_{pol} in LrH^+ can be attributed to its smaller reduced mass. Therefore, LrH^+ may not be as suitable as the other two considered candidates, but it can also be considered in an experiment if any alternative technique suitable to measure EDM in this ion can be found.

We now turn our attention to estimating the production rates of Lr molecules for an EDM experiment. We propose to use the RIKEN heavy-ion linear accelerator (RILAC) facility because a high-intensity ion beam is readily available to produce the atoms of interest. As for ^{256}Lr production, we propose the $^{209}\text{Bi}(^{48}\text{Ca}, 1n)$ reaction as a possible candidate, for which a production cross section of 60 nb has been reported [65], although it is necessary to have a stable supply of ^{48}Ca . As explained in Ref. [66], the $^{249}\text{Cf}(^{11}\text{B}, 4n)$ reaction was employed in the single-ion beam production of ^{256}Lr at JAEA due to its relatively high cross section of 122 nb. The ^{249}Cf target material is, however, radioactive and too rare to prepare a target sufficiently large to apply to a beam from RILAC. On the other hand, ^{209}Bi is stable and easy to handle when making a target with a large area. A typical target thickness is $300 \mu\text{g cm}^{-2}$ [67]. The RILAC facility can typically provide a $3\text{-p}\mu\text{A}$ ^{48}Ca beam. In this situation, Lr atoms can be produced at a rate of one atom per second. In the case that the GAs-filled Recoil Ion Separator (GARIS) is applied to mass separation and single-ion beam production, a transparent efficiency of 50% is expected [68]. In addition, in preliminary experiments at JAEA, about 20% of Lr can be converted to LrO. Thus, we estimate $N \approx 0.1$ molecule per second. This means that only a molecular beam of about one atom per minute could be produced, which presents major challenges for experiments with neutral molecules. On the other hand, molecular ions such as LrF^+ and LrH^+ can be efficiently guided and trapped by electromagnetic fields, enabling experiments even with just a single molecular ion.

V. CONCLUSION

We have considered the prospects of the CP -violating electron EDM and the nucleus-electron S-PS searches in LrF^+ , LrH^+ , and LrO. We found that bound states with a stable minimum do occur in the chosen molecular systems. We reported calculations of \mathcal{E}_{eff} , W_s , and μ for the aforementioned molecules using the relativistic coupled-cluster method. We analyzed the importance of correlation effects for the properties in these three systems. We observed that the values of \mathcal{E}_{eff} for the three superheavy molecules are about

3–4 times larger than those of other molecules on which EDM experiments are being performed. Similarly, the W_s values were found to be more than 3 times larger. By analyzing the Woods-Saxon model to account for the nuclear charge-density distribution, we found that the calculated the S-PS interaction coefficients are very sensitive to the diffuse surface interactions in the superheavy Lr nucleus and need to be accounted for to get an accurate estimate of the W_s values. We discussed a feasible pathway to produce Lr atoms, which are necessary for the creation of superheavy molecules containing these atoms. We also studied the properties of LrF^+ and LrH^+ molecules and their potential for future single-ion experiments. Our precisely estimated bond lengths and μ values for the LrF^+ , LrH^+ , and LrO molecules could also be useful for guiding other experimental setups using these superheavy molecules.

ACKNOWLEDGMENTS

Most of the calculations reported in this work were performed using the Vikram-100 high-performance computing facility at PRL, Ahmedabad. The rest of the calculations were carried out on the National Supercomputing Mission's (NSM) computing resource "PARAM Siddhi-AI" at C-DAC Pune, which is implemented by C-DAC and supported by the Ministry of Electronics and Information Technology (MeitY) and the Department of Science and Technology (DST), Government of India. This work was partially supported by the Office of Nuclear Physics, U.S. Department of Energy, under Grants No. DE-SC0021176 and No. DE-SC0021179. Y.S. acknowledges JSPS KAKENHI Grant No. JP19H05601. M.A. acknowledges JSPS KAKENHI Grants No. JP19K22171, No. JP20H01929, and No. JP21H01864.

-
- [1] V. Andreev, D. G. Ang, D. DeMille, J. M. Doyle, G. Gabrielse, J. Haefner, N. R. Hutzler, Z. Lasner, C. Meisenhelder, B. R. O'Leary, C. D. Panda, A. D. West, E. P. West, and X. Wu (ACME Collaboration), *Nature (London)* **562**, 355 (2018).
- [2] L. V. Skripnikov, A. N. Petrov, and A. V. Titov, *J. Chem. Phys.* **139**, 221103 (2013).
- [3] E. R. Meyer, J. L. Bohn, and M. P. Deskevich, *Phys. Rev. A* **73**, 062108 (2006).
- [4] P. Aggarwal, H. L. Bethlem, A. Borschevsky, M. Denis, K. Esaja, P. A. B. Haase, Y. Hao, S. Hoekstra, K. Jungmann, T. B. Meijknecht, M. C. Mooij, R. G. E. Timmermans, W. Ubachs, L. Willmann, and A. Zapara (NL-EDM Collaboration), *Eur. Phys. J. D* **72**, 197 (2018).
- [5] A. C. Vutha, M. Horbatsch, and E. A. Hessels, *Atoms* **6**, 3 (2018).
- [6] D. M. Kara, I. J. Smallman, J. J. Hudson, B. E. Sauer, M. R. Tarbutt, and E. A. Hinds *et al.*, *New J. Phys.* **14**, 103051 (2012).
- [7] A. Sunaga, M. Abe, M. Hada, and B. P. Das, *Phys. Rev. A* **99**, 062506 (2019).
- [8] V. S. Prasanna, A. C. Vutha, M. Abe, and B. P. Das, *Phys. Rev. Lett.* **114**, 183001 (2015).
- [9] A. Sunaga, V. S. Prasanna, M. Abe, and M. Hada, and B. P. Das, *Phys. Rev. A* **99**, 040501(R) (2019).
- [10] I. Kozyryev and N. R. Hutzler, *Phys. Rev. Lett.* **119**, 133002 (2017).
- [11] A. Zakharova and A. Petrov, *Phys. Rev. A* **103**, 032819 (2021).
- [12] R. Mitra, V. S. Prasanna, B. K. Sahoo, N. Hutzler, M. Abe, and B. P. Das, *Atoms* **9**, 7 (2021).
- [13] Z. Yang, J. Li, Q. Lin, L. Xu, H. Wang, T. Yang, and J. Yin, *Phys. Rev. A* **99**, 032502 (2019).
- [14] N. Yamanaka, B. K. Sahoo, N. Yoshinaga, and T. Sato, K. Asahi, and B. P. Das, *Eur. Phys. J. A* **53**, 54 (2017).
- [15] T. E. Chupp, P. Fierlinger, M. J. Ramsey-Musolf, and J. T. Singh, *Rev. Mod. Phys.* **91**, 015001 (2019).
- [16] C. Cesarotti, Q. Lu, Y. Nakai, A. Parikha, and M. Reece, *J. High Energy Phys.* **05** (2019) 059.
- [17] A. M. Kazarian, S. V. Kuzmin, and M. E. Shaposhnikov, *Phys. Lett. B* **276**, 131 (1992).
- [18] K. Fuyuto, J. Hisano, and E. Senaha, *Phys. Lett. B* **755**, 491 (2016).
- [19] P. G. H. Sandars, *Phys. Lett.* **22**, 290 (1966).
- [20] O. P. Sushkov and V. V. Flambaum, *J. Exp. Theor. Phys.* **48**, 608 (1978).
- [21] V. V. Flambaum, *Sov. J. Nucl. Phys.* **24**, 199 (1976).
- [22] V. V. Flambaum and I. B. Khriplovich, *J. Exp. Theor. Phys.* **62**, 872 (1985).
- [23] R. F. Garcia Ruiz *et al.*, *Nature (London)* **581**, 396 (2020).
- [24] S. M. Udrescu *et al.*, *Phys. Rev. Lett.* **127**, 033001 (2021).
- [25] T. A. Isaev, *Phys. Usp.* **63**, 289 (2020).
- [26] T. A. Isaev and R. Berger, [arXiv:1302.5682](https://arxiv.org/abs/1302.5682).
- [27] A. Sunaga, V. S. Prasanna, M. Abe, M. Hada, and B. P. Das, *Phys. Rev. A* **98**, 042511 (2018).
- [28] K. Gaul, S. Marquardt, T. Isaev, and R. Berger, *Phys. Rev. A* **99**, 032509 (2019).
- [29] T. K. Sato *et al.*, *Nature (London)* **520**, 209 (2015).
- [30] P. Yu and N. R. Hutzler, *Phys. Rev. Lett.* **126**, 023003 (2021).
- [31] M. Fan, C. A. Holliman, X. Shi, H. Zhang, M. W. Straus, X. Li, S. W. Buechele, and A. M. Jayich, *Phys. Rev. Lett.* **126**, 023002 (2021).
- [32] W. B. Cairncross, D. N. Gresh, M. Grau, K. C. Cossel, T. S. Roussy, Y. Ni, Y. Zhou, J. Ye, and E. A. Cornell, *Phys. Rev. Lett.* **119**, 153001 (2017).
- [33] T. Naito, R. Akashi, H. Liang, and S. Tsuneyuki, *J. Phys. B* **53**, 215002 (2020).
- [34] C. Bouchiat, *Phys. Lett. B* **57**, 284 (1975).
- [35] B. P. Das, in *Aspects of Many-Body Effects in Molecules and Extended Systems*, edited by D. Mukherjee (Springer, Berlin, 1989), p. 411.
- [36] E. Lindroth, B. W. Lynn, and P. G. H. Sandars, *J. Phys. B* **22**, 559 (1989).
- [37] M. G. Kozlov, *Phys. Lett. A* **130**, 426 (1988).
- [38] M. Born and J. R. Oppenheimer, *Ann. Phys. (Berlin, Ger.)* **389**, 457 (1927).
- [39] R. F. Bishop and H. G. Kummel, *Phys. Today* **40**(3), 52 (1987).
- [40] J. Cizek, *Adv. Chem. Phys.* **14**, 35 (1969).
- [41] I. Shavitt and R. J. Bartlett, *Many-Body Methods in Chemistry and Physics: MBPT and Coupled-Cluster Theory* (Cambridge University Press, Cambridge, 2009).
- [42] T. Saue *et al.*, DIRAC, a relativistic *ab initio* electronic structure program, release DIRAC18, 2018, <http://www.diracprogram.org>.

- [43] L. Visscher, T. J. Lee, and K. G. Dyall, *J. Chem. Phys.* **105**, 8769 (1996).
- [44] K. G. Dyall, *Theor. Chem. Acc.* **117**, 491 (2007).
- [45] T. Yanai, H. Nakano, T. Nakajima, T. Tsuneda, S. Hirata, Y. Kawashima, Y. Nakao, M. Kamiya, H. Sekino, and K. Hirao, in *UTCHEM: A Program for Ab Initio Quantum Chemistry*, edited by G. Goos, J. Hartmanis, and J. van Leeuwen, Lecture Notes in Computer Science Vol. 2660 (Springer, Berlin, 2003), p. 84.
- [46] T. Yanai, T. Nakajima, Y. Ishikawa, and K. Hirao, *J. Chem. Phys.* **114**, 6526 (2001); **116**, 10122 (2002).
- [47] L. Visscher *et al.*, DIRAC, a relativistic *ab initio* electronic structure program, release DIRAC08, 2008, <http://dirac.chem.sdu.dk>.
- [48] V. S. Prasanna, B. K. Sahoo, M. Abe, and B. P. Das, *Symmetry* **12**, 811 (2020).
- [49] C. Zhang, X. Zheng, and L. Cheng, *Phys. Rev. A* **104**, 012814 (2021).
- [50] L. V. Skripnikov, *J. Chem. Phys.* **147**, 021101 (2017).
- [51] A. Sunaga, M. Abe, M. Hada, and B. P. Das, *Phys. Rev. A* **93**, 042507 (2016).
- [52] H. S. Nataraj, B. K. Sahoo, B. P. Das, and D. Mukherjee, *Phys. Rev. Lett.* **101**, 033002 (2008).
- [53] B. K. Sahoo, B. P. Das, R. K. Chaudhuri, D. Mukherjee, and E. P. Venugopal, *Phys. Rev. A* **78**, 010501(R) (2008).
- [54] T. Fleig and L. V. Skripnikov, *Symmetry* **12**, 498 (2020).
- [55] N. Shitara, N. Yamanaka, B. K. Sahoo, T. Watanabe, and B. P. Das, *J. High Energy Phys.* **02** (2021)124.
- [56] V. S. Prasanna, M. Abe, V. M. Bannur, and B. P. Das, *Phys. Rev. A* **95**, 042513 (2017).
- [57] L. Visscher and K. G. Dyall, *At. Data Nucl. Data Tables* **67**, 207 (1997).
- [58] D. Andrae, *Phys. Rep.* **336**, 413 (2000).
- [59] E. Rost, *Phys. Lett. B* **26**, 184 (1968).
- [60] M. R. Pahlavani and S. A. Alavi, *Commun. Theor. Phys.* **58**, 739 (2012).
- [61] G. Estevez and L. B. Bhuiyan, *Am. J. Phys.* **53**, 450 (1985).
- [62] V. M. Shabaev, M. Tomaselli, T. Kühn, A. N. Artemyev, and V. A. Yerokhin, *Phys. Rev. A* **56**, 252 (1997).
- [63] K. Yanase (private communication).
- [64] B. K. Sahoo, R. Chaudhuri, B. P. Das, and D. Mukherjee, *Phys. Rev. Lett.* **96**, 163003 (2006).
- [65] S. Antalic, F. P. Heßberger, D. Ackermann, S. Heinz, S. Hofmann, Z. Kalaninová, B. Kindler, J. Khuyagbaatar, I. Kojouharov, P. Kuusiniemi, M. Leino, B. Lommel, R. Mann, K. Nishio, Š. Šáro, B. Streicher, B. Sulignano, and M. Venhart, *Euro. Phys. J. A* **47**, 62 (2011).
- [66] N. Sato, T. K. Sato, M. Asai, A. Toyoshima, K. Tsukada, Z. J. Li, K. Nishio, Y. Nagame, M. Schädel, H. Haba, S. Ichikawa, and H. Kikunaga, *Radiochim. Acta* **102**, 211 (2014).
- [67] D. Kaji, K. Morimoto, A. Yoneda, H. Hasebe, A. Yoshida, H. Haba, S. Goto, H. Kudo, and K. Morita, *Nucl. Instrum. Method. A* **590**, 198 (2008).
- [68] K. Morita, *Nucl. Phys. A* **944**, 30 (2015).